

<https://doi.org/10.1038/s43856-025-01032-0>

Reply to: “The non-cytotoxic small molecule NPB does not inhibit BAD phosphorylation and forms colloidal aggregates”

Xi Zhang¹, Basappa Basappa², Peter E. Lobie^{1,3}✉ & Vijay Pandey³✉REPLYING TO Githaka et al. *Communications Medicine* <https://doi.org/10.1038/s43856-022-00142-3> (2025)

In the published work¹, a previously described phospho-BADSer99 (pBADS99) small-molecule inhibitor, NPB², was used to demonstrate that combined pBADS99-PARP inhibition synergistically enhanced apoptosis in epithelial ovarian carcinoma cells by increasing DNA damage and impairing PARP-induced DNA repair¹. In response to this work^{1,2}, Githaka et al.³ submitted a “Matters Arising”. However, it is our opinion that the conclusion of the “Matters Arising” that “NPB forms large colloidal aggregates that are incompatible with the proposed mechanism of action” has not been causally established; the attempts in the “Matters Arising” to replicate the previously reported results^{1,2,4–6} are preliminary and also contain multiple technical considerations that preclude the conclusions made.

The NPB provided by the University of Mysore (UM) to Githaka et al. was also retested in the Shenzhen laboratory and produced a dose-dependent decrease in cell viability (Fig. 1A) and a corresponding decrease in pBADS99 (Fig. 1B), consistent with previously published data^{1,2,5}. The specificity of the antibody used to detect pBADS99 herein has been demonstrated by the use of BAD deletion, depletion, or expression^{1,5}, murine badS136A⁴ or human BADS99A expression vectors^{1,5}, pharmacological modulation^{1,2,4–6}, and by homology-directed repair of human BADS99 to BADA99⁷. Despite claims to replicate our data, Githaka et al.³ among multiple other issues, used a pBADS99 antibody from a different commercial source (supplementary information (SI) 4 file of ref. 8 and ref. 3). This is of concern given the near-complete uniformity of BAD expression and phosphorylation over time in culture observed by Githaka et al. (SI3c³). In contrast, it has been reported that BAD expression^{9,10} pathways phosphorylating BAD^{9,11} and BAD phosphorylation^{6,7,12} and function^{11,13–15} are dynamically regulated by cell density/confluence, as observed in Fig. 1C herein. Furthermore, the “time course” presented in the “Matters Arising” SI3c lacks corresponding temporal controls for vehicle treatment. Hence, independent of NPB, Githaka et al. have failed to replicate the fundamental cell-based assays.

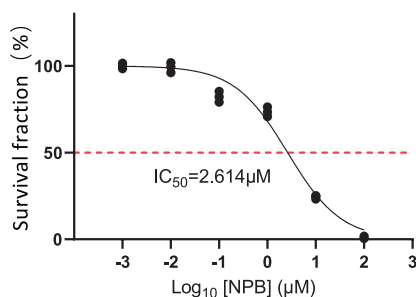
We have previously published a series of NPB analogues, some of which retain the ability to inhibit pBADS99 and decrease cell viability¹⁶.

Utilizing the same “aggregator advisor” platform (<https://advisor.bkslab.org>), the majority of the NPB analogues were labelled “suspicious of aggregation” (Supplementary Data (SD) 1). No significant correlation emerged between the assigned aggregator advisor categories and the $\log P$ nor IC_{50} values of the NPB series of compounds¹⁶ (Supplementary Fig. (SF) 1). Furthermore, compounds used clinically, including BH3 mimetics, displayed varying aggregation designations on the platform, including “highly suspicious of aggregation” (SD1). Indeed, the platform itself states that “prediction of aggregation is difficult” and that the platform does not predict aggregation (Supplementary Note). Furthermore, multiple other FDA-approved drugs such as Fulvestrant, Sorafenib, and Crizotinib have been demonstrated to aggregate yet retain on-target activity¹⁷.

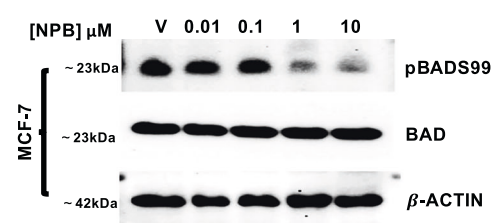
Githika et al.³ report a critical aggregation concentration (CAC) for the commercial NPB of 0.1 μM , which is low given published reports for other molecules¹⁷ and considering that small molecules generally aggregate in a higher micromolar range (Table 1 of ref. 17). The detailed experimental conditions under which this CAC value was generated are not provided, yet the CAC is an arbitrary number dramatically influenced by variables such as pH, temperature, ionic strength, DMSO and protein/serum-concentrations^{17,18}. The CAC value in “Matters Arising” is inconsistent with the previously reported aqueous solubility of NPB generated by an outside service provider of $38.7 \pm 2.6 \mu M$ (3 h) at $22.5 \pm 2.5 ^\circ C$,² as at concentrations above the CAC, NPB should be sequestered to an aggregate¹⁹. The full technical report of this data is now provided in Supplementary Method (SM) 1. CAC values have usually been generated in a defined buffer^{18,19} but may also be calculated in serum-containing media¹⁸. Hence, determination of the NPB CAC under the cell-based assay conditions utilized should be germane to address the lack of NPB activity observed by Githika et al.³. NPB colloidal aggregation would not explain the cellular response to NPB observed in our laboratory, as colloidal aggregates do not enter the cell²⁰, rapidly form a protein corona^{17,20} which impedes cellular contact^{19,20}, and sequester chemical monomers that may otherwise be active; thus, actually producing false negatives in cell-based assays¹⁷. Furthermore, the “enzymes”

¹Shenzhen Bay Laboratory, Shenzhen, Guangdong, China. ²Laboratory of Chemical Biology, Department of Studies in Organic Chemistry, University of Mysore, Manasagangotri, Mysore, Karnataka, India. ³Institute of Biopharmaceutical and Health Engineering, Tsinghua Shenzhen International Graduate School, Tsinghua University, Shenzhen, People's Republic of China. ✉e-mail: pelobie@sz.tsinghua.edu.cn; vijay.pandey@sz.tsinghua.edu.cn

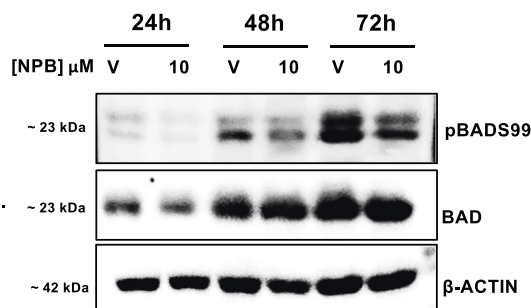
A. Cell viability



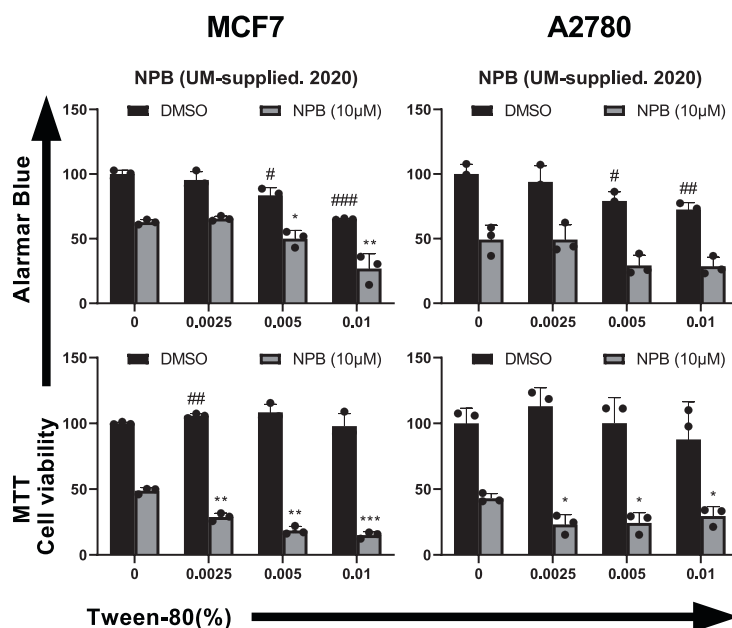
B. Western blot analysis



C. Western blot analysis



D. Cell viability



E. 3D Matrigel assay

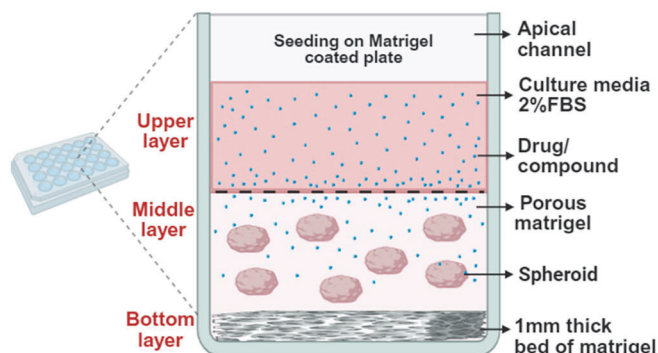


Fig. 1 | NPB inhibits BAD Serine (S) 99 phosphorylation and reduces cell survival. **A** Cell viability assay: Dose-response curve of University of Mysore (UM) supplied NPB in the year 2020. The cell survival fraction (%) was measured at 72 h ($n = 3$). The IC_{50} value was calculated using GraphPad Prism (7.0). **B** Western blot: The pBADs99 and BAD protein levels in MCF-7 cells treated with NPB as indicated for 48 h and evaluated using WB analysis. **C** The pBADs99 and BAD protein levels in MCF-7 cells treated with the NPB dose as indicated for 24, 48, or 72 h and evaluated using WB analysis. V=vehicle. β -ACTIN was used as an input control. **D** The non-

ionic detergent Tween-80 enhances the efficacy of NPB. Cell viability (%) was analyzed by using MTT and Alamar Blue assays. Data represent mean \pm SD ($n = 3$). * ($\#$) $P < 0.05$, ** ($\#\#$) $P < 0.01$, and *** ($\#\#\#$) $P < 0.001$ compared. P -value in the t -test compared to TWEEN-80 is denoted as #, P -value in the t -test compared to NPB (10 μ M) with 0% TWEEN-80 is denoted as *. UM: University of Mysore. **E** Live/dead assay performed using 3D Matrigel culture assays previously performed^{1,3,5,10-12}. The illustration was generated using the online platform BioRender.com. The unprocessed western blot images are represented in Supplementary Fig. 3.

referred to in the “Matters Arising” as being impacted by aggregation are simply enzymes used in cell-free biochemical assays²¹, as chemical aggregates absorb and denature proteins on their surface; hence, the ability of aggregates to produce false positive hits in high-throughput drug screens for ligand-protein interaction²¹. If loss of cell viability in our assays was due to NPB fibril (or aggregate) formation as was implied³, then the observed effect of NPB in the Shenzhen laboratory should be reduced by the addition of non-ionic detergent in assays^{17,22}, yet it was increased (Fig. 1D). The optimal doses of Tween-80 for retention of MCF-7 and A2780 cell viability were also assessed (SF2A). Additionally, Matrigel is largely impermeable to even small nanoparticles²³ and NPB activity is maintained in 3D Matrigel culture^{1,2,4,5} through a Matrigel barrier separating cell colonies and NPB in media (Fig. 1E). Furthermore, in multiple xenograft-based models, NPB was

injected intraperitoneally, anatomically separated from the xenograft, and yet displayed potent in vivo activity and target engagement, as demonstrated by decreased BADs99 phosphorylation in the xenograft sample^{1,2,4-7,12}.

It is not unusual to observe that the “sensitivity” of assays in different laboratories is dissimilar, and the explanations for this may be multiple. As an example, the IC_{50} values of ABT-199 in MCF-7 cells exhibit a notable variability across different laboratories, spanning more than 150-fold (0.27 to 30 μ M) (SD1&SF2B). NPB is clearly not a potent molecule in in vitro assays^{1,2,4}, and even other potent small-molecule inhibitors of major signaling pathways, such as the SOS-1 inhibitors generated by Boehringer Ingelheim (BI-3406) or Bayer (BAY293), have been reported by some investigators to lack activity in 2D cell viability assays²⁴. In contrast, multiple independent operators in the Shenzhen laboratory observed the activity of

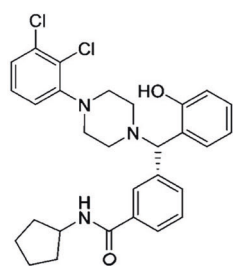
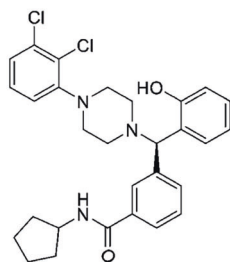
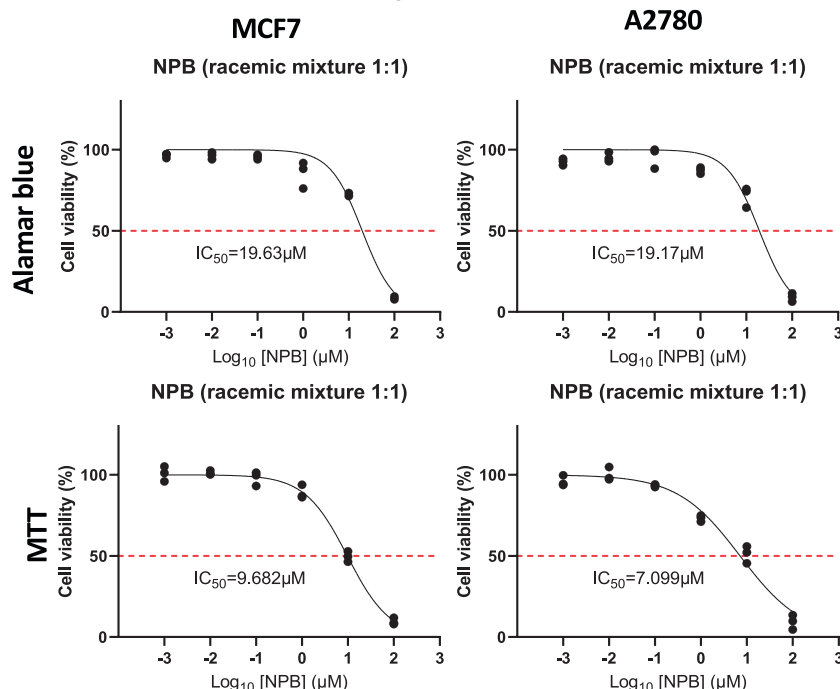
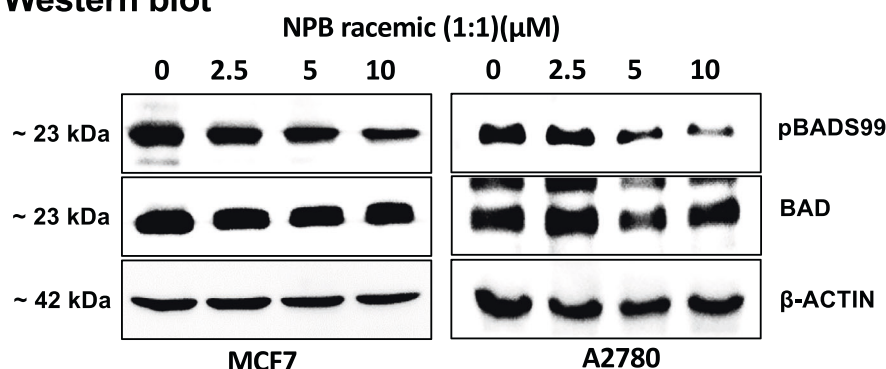
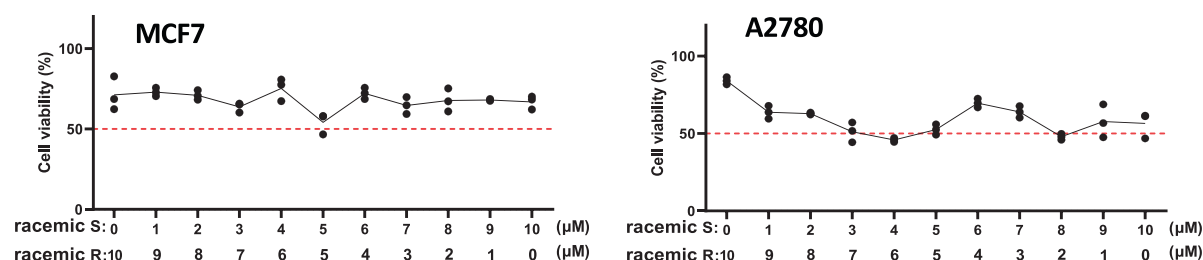
A. NPB enantiomers (S/R)**NPB enantiomer 1****NPB enantiomer 2****B. Dose-response analysis****C. Western blot****D. Cell viability**

Fig. 2 | Enantiomer-specific effects of NPB on cancer cell viability and BADS99 dephosphorylation. **A** NPB enantiomer. S (levorotatory) and R (dextrorotatory). **B** Cell viability assay: Dose-response curve of NPB. The cell survival fraction (%) was measured at 72 h ($n = 3$). The IC₅₀ value was calculated using GraphPad Prism (7.0). **C** Western blot: The levels of pBADS99 and BAD protein in MCF-7 or A2780 cells

treated with doses of NPB-racemic mix (1:1) as indicated for 72 h were evaluated using WB analysis. β-ACTIN was used as an input control. **D** Cell viability (%) of MCF-7 and A2780 cells was measured by AlamarBlue assay after 72 h of treatment with variable ratios of NPB enantiomers ($n = 3$). The unprocessed western blot images are represented in Supplementary Fig. 3.

BI-3406 in 2D cell viability assays (SF2C), and a different laboratory has also observed the activity of BAY293 in 2D culture²⁵. Hence, the use of more appropriate controls, such as inhibitors of the BCL-2 family (BH3 mimetics), may better assist in gauging the sensitivity of assays used by Githaka et al. (for example, see SF2B). NPB is a hydrophobic molecule with limited

solubility², and the lack of NPB activity observed by Githaka et al. is likely due to mundane differences in cell culture materials or process, failing to sufficiently optimize NPB solubility.

Finally, NPB is a chiral molecule (Fig. 2A, SM2), and different synthetic processes may alter the enantiomeric proportions or impurities in a racemic

mixture. Analysis of the basic ^1H NMR of the Axon-Medchem NPB preparation in ref. 3 indicates potential contamination²⁶. This is evidenced by the spectral data obtained in DMSO and CDCl_3 , which are different. In the CDCl_3 solvent, peaks with delta values of 2.2, 4.4, and 4.6 are observed, which differ from those in DMSO, appearing at 1.8, 4.2, and 4.8, respectively. In addition, the mass spectra showed a number of fragmentation peaks apart from molecular ion peaks. We therefore contracted an independent third party (WuXi AppTec, Shanghai, China) to synthesize and purify S and R enantiomers of NPB (see SM2). Enantiomers were prepared at 98% purity and mixed in a 1:1 ratio to generate a racemic mixture as used previously². Consistent with previous results using UM-provided NPB, the WuXi AppTec racemic mix of NPB demonstrated a dose-dependent decrease in BADS99 phosphorylation and cell viability (Fig. 2B, C). Systematic manipulation of the enantiomer ratio also did not significantly alter the cell viability responses observed (Fig. 2D).

Previously published, comprehensive and detailed data demonstrate the functional efficacy of NPB in vitro, ex vivo, and in vivo^{1,2,4,5}. Multiple scientists working in different laboratories and using different synthetic batches of NPB have observed the activity of NPB in various assays^{1,2,4-6}. Whereas NPB is a hydrophobic molecule and may possess a tendency to aggregate, we have reported that the observed NPB efficacy largely depends on the cellular presence of BAD and BADS99 in particular^{1,2,4-7,12}. We also do not deny the possibility of NPB polypharmacology, as is common in small-molecule targeted therapeutics^{27,28}; and indeed, this possibility was indicated by the published analysis² in which NPB was predicted to bind to multiple proteins in addition to BAD (SF2). It should also be noted that due to the reversible nature of aggregates, aggregation may also be considered advantageous^{18,29} with aggregates potentially acting as a drug reservoir and improving pharmacokinetic/delivery parameters. However, NPB suffers from poor oral bioavailability²; hence, it serves only as an exemplar to develop more potent and orally available analogues inhibiting BADS99 phosphorylation^{7,12}.

Materials and methods

NPB reconstitution

5.23 mg of NPB powder (from either UM or WuXi AppTec, Shanghai; Project number: QHSZG-20230214, SM2) was diluted in 1000 μL of DMSO (molecular biology grade, Sigma-Aldrich, D8418, Germany) for a stock concentration of 10 mM as described in SM3 and as previously published^{1,2,4-6}. No issues were noted with compound aggregation in the NPB preparations during cell culture experiments.

Cell culture and in vitro assays

The detailed information for cell lines, culturing conditions, cell viability (as assessed by Alamar Blue and MTT), and Western blot is described in SM3&SF3 and as previously published^{1,2,5-7,12}.

Data availability

The data supporting the findings of this study are available from the authors upon reasonable request; see the author contributions for specific data sets. Supplementary Data 2 contains the source data for Figs. 1, 2, and Supplementary Fig. 2.

Received: 9 April 2023; Accepted: 4 July 2025;

Published online: 30 July 2025

References

- Zhang, X. et al. Combined inhibition of BADSer99 phosphorylation and PARP ablates models of recurrent ovarian carcinoma. *Commun. Med.* **2**, 82 (2022).
- Pandey, V. et al. Discovery of a small-molecule inhibitor of specific serine residue BAD phosphorylation. *Proc. Natl Acad. Sci. USA* **115**, E10505–E10514 (2018).
- Githaka, J. M. et al. The non-cytotoxic small molecule NPB does not inhibit BAD phosphorylation and forms colloidal aggregates. *Commun. Med.* **5**, 166 (2025).
- Wang, Y. et al. Pharmacological inhibition of BAD Ser99 phosphorylation enhances the efficacy of cisplatin in ovarian cancer by inhibition of cancer stem cell-like behavior. *ACS Pharm. Transl. Sci.* **3**, 1083–1099 (2020).
- Zhang, X. et al. Inhibition of BAD-Ser99 phosphorylation synergizes with PARP inhibition to ablate PTEN-deficient endometrial carcinoma. *Cell Death Dis.* **13**, 558 (2022).
- Wang, L. et al. Combining mitomycin C with inhibition of BAD phosphorylation enhances apoptotic cell death in advanced cervical cancer. *Transl. Oncol.* **49**, 102103 (2024).
- Tan, Y. Q. et al. Vertical pathway inhibition of receptor tyrosine kinases and BAD with synergistic efficacy in triple negative breast cancer. *NPJ Precis. Oncol.* **8**, 8 (2024).
- Githaka, J. M. et al. BAD regulates mammary gland morphogenesis by 4E-BP1-mediated control of localized translation in mouse and human models. *Nat. Commun.* **12**, 2939 (2021).
- Ishibe, S. et al. Cell confluence regulates hepatocyte growth factor-stimulated cell morphogenesis in a beta-catenin-dependent manner. *Mol. Cell Biol.* **26**, 9232–9243 (2006).
- Scheid, M. P., Schubert, K. M. & Duronio, V. Regulation of bad phosphorylation and association with Bcl-x(L) by the MAPK/Erk kinase. *J. Biol. Chem.* **274**, 31108–31113 (1999).
- Datta, S. R. et al. Survival factor-mediated BAD phosphorylation raises the mitochondrial threshold for apoptosis. *Dev. Cell* **3**, 631–643 (2002).
- Tan, Y. Q. et al. Concurrent inhibition of pBADS99 synergistically improves MEK inhibitor efficacy in KRAS(G12D)-mutant pancreatic ductal adenocarcinoma. *Cell Death Dis.* **15**, 173 (2024).
- Fernando, R. I. *BAD is a Central Player in Cell Death and Cell Cycle Regulation in Breast Cancer Cells*. (University of Tennessee, Knoxville, 2004).
- Pennington, K. L. et al. The dynamic and stress-adaptive signaling hub of 14-3-3: emerging mechanisms of regulation and context-dependent protein-protein interactions. *Oncogene* **37**, 5587–5604 (2018).
- Boac, B. M. et al. Expression of the BAD pathway is a marker of triple-negative status and poor outcome. *Sci. Rep.* **9**, 17496 (2019).
- Girimanchanaika, S. S. et al. Investigation of NPB analogs that target phosphorylation of BAD-Ser99 in human mammary carcinoma cells. *Int. J. Mol. Sci.* **22**, 11002 (2021).
- Owen, S. C. et al. Colloidal aggregation affects the efficacy of anticancer drugs in cell culture. *ACS Chem. Biol.* **7**, 1429–1435 (2012).
- Ganesh, A. N. et al. Colloidal drug aggregate stability in high serum conditions and pharmacokinetic consequence. *ACS Chem. Biol.* **14**, 751–757 (2019).
- Owen, S. C. et al. Colloidal drug formulations can explain “bell-shaped” concentration-response curves. *ACS Chem. Biol.* **9**, 777–784 (2014).
- Ganesh, A. N. et al. Colloidal aggregation: from screening nuisance to formulation nuance. *Nano Today* **19**, 188–200 (2018).
- Coan, K. E. et al. Promiscuous aggregate-based inhibitors promote enzyme unfolding. *J. Med. Chem.* **52**, 2067–2075 (2009).
- Julien, O. et al. Unraveling the mechanism of cell death induced by chemical fibrils. *Nat. Chem. Biol.* **10**, 969–976 (2014).
- Van Zundert, I., Fortuni, B. & Rocha, S. From 2D to 3D cancer cell models—the enigmas of drug delivery research. *Nanomaterials* **10**, 2236 (2020).
- Hofmann, M. H. et al. BI-3406, a potent and selective SOS1-KRAS interaction inhibitor, is effective in KRAS-driven cancers through combined MEK inhibition. *Cancer Discov.* **11**, 142–157 (2021).
- Hillig, R. C. et al. Discovery of potent SOS1 inhibitors that block RAS activation via disruption of the RAS-SOS1 interaction. *Proc. Natl Acad. Sci. USA* **116**, 2551–2560 (2019).
- Fulmer, G. R. et al. NMR chemical shifts of trace impurities: common laboratory solvents, organics, and gases in deuterated solvents

- relevant to the organometallic chemist. *Organometallics* **29**, 2176–2179 (2010).
27. Hafner, M. et al. Multiomics profiling establishes the polypharmacology of FDA-approved CDK4/6 inhibitors and the potential for differential clinical activity. *Cell Chem. Biol.* **26**, 1067–1080.e8 (2019).
28. Antolin, A. A. et al. The kinase polypharmacology landscape of clinical PARP inhibitors. *Sci. Rep.* **10**, 2585 (2020).
29. Ganesh, A. N. et al. Leveraging colloidal aggregation for drug-rich nanoparticle formulations. *Mol. Pharm.* **14**, 1852–1860 (2017).

Author contributions

X.Z., P.E.L., and V.P. designed the research; X.Z. performed in vitro assays; B.B. synthesized NPB; X.Z., B.B., P.E.L., and V.P. analyzed the data and wrote the manuscript. All authors have read and approved the manuscript for publication.

Competing interests

V.P., B.B., and P.E.L. are listed as inventors on a patent application (and all derivatives) for NPB, which is used in this work (WO/2019/194520). P.E.L. is an equity holder in Sinotar Pharmaceuticals Ltd, which currently holds the license for this patent. X.Z. declare no competing interests.

Additional information

Supplementary information The online version contains supplementary material available at <https://doi.org/10.1038/s43856-025-01032-0>.

Correspondence and requests for materials should be addressed to Peter E. Lobie or Vijay Pandey.

Reprints and permissions information is available at <http://www.nature.com/reprints>

Publisher's note Springer Nature remains neutral with regard to jurisdictional claims in published maps and institutional affiliations.

Open Access This article is licensed under a Creative Commons Attribution-NonCommercial-NoDerivatives 4.0 International License, which permits any non-commercial use, sharing, distribution and reproduction in any medium or format, as long as you give appropriate credit to the original author(s) and the source, provide a link to the Creative Commons licence, and indicate if you modified the licensed material. You do not have permission under this licence to share adapted material derived from this article or parts of it. The images or other third party material in this article are included in the article's Creative Commons licence, unless indicated otherwise in a credit line to the material. If material is not included in the article's Creative Commons licence and your intended use is not permitted by statutory regulation or exceeds the permitted use, you will need to obtain permission directly from the copyright holder. To view a copy of this licence, visit <http://creativecommons.org/licenses/by-nc-nd/4.0/>.

© The Author(s) 2025